

FINITE ELEMENT ANALYSIS OF THERMOELASTIC INSTABILITY OF A RECTANGULAR BLOCK ON A RIGID WALL

Taein Yeo
Dept. of Automotive Engineering

<Abstract>

The steady-state conduction of heat across an interface between two contacting bodies can become unstable as a result of the interaction between thermoelastic distortion and a pressure-dependent thermal contact resistance. Analytical solutions for the stability boundary have been obtained for simple systems using perturbation methods, but become prohibitively complex for finite geometries. This paper presents a finite element formulation of the perturbation method, in which the linearity of the governing equations is exploited to obtain separated-variable solutions for the perturbation with exponential variation in time. The problem is thus reduced to a linear eigenvalue problem with the exponential growth rate appearing as the eigenvalue. Stability of the system requires that all eigenvalues have negative real part. The method is tested against an analytical solution of the two-dimensional problem of a strip in contact with a rigid wall. Excellent results are obtained for the stability boundary even with a relatively coarse discretization.

강체와 열탄성적 접촉하에 있는 사각블럭의 불안정성에 대한 유한요소해석

여태인
자동차공학과

<요 약>

두 물체의 접촉면 사이의 정상상태의 열전달은 열변형을 일으키고 그결과 나타나는 접촉압력의 변화는 열접촉저항 및 열전달을 변화시켜 전체 시스템을 불안정하게 할 수 있다.

섭동법에 의한 이론적 해석방법은 단순한 시스템에 대하여는 가능하지만 유한한 길이의 기하학적 형상을 가진 시스템에 대하여는 매우 어려워진다. 본논문에서는 강체와 열탄성적 접촉을 하고있는 사각블럭의 안정성을 판정하기위해 시간에 따라 지수적으로 변화하는 변수분리 형태의 섭동을 가정하여 지배방정식들을 유한요소식화 하였다. 그결과 지수증가율에 대한 선형 고유치 문제를 얻을 수 있으며, 시스템은 모든 고유치가 음의 실수부를 가질때 안정하다. 수치적인 해석결과를 강체인 벽과 열탄성적인 접촉을 하고있는 스트립의 이론적 해석결과와 비교하여 제안한 유한요소법의 타당성을 보였다.

1. Introduction

The steady-state conduction of heat across an interface between two contacting bodies can become unstable as a result of thermoelastic effects. Briefly, the thermal distortion of the bodies affects the contact pressure distribution and this in turn affects the heat conduction problem by changing the thermal contact resistance at the interface which is generally pressure-sensitive.

Early investigations of thermoelastic contact stability were restricted to one-dimensional systems such as a rod contacting a rigid wall (Barber *et al.*, 1980) or axisymmetric concentric cylinders of similar materials (Barber (1986)). Barber and Zhang (1988) investigated the more complex one-dimensional system of two contacting rods of dissimilar materials and also developed a numerical solution for the transient behavior.

The simplest two-dimensional problem is that of two elastic half-planes in

contact at a common interface. Barber (1987) adapted the methods of Dow and Burton (1972) and Richmond and Huang (1977) for related problems to examine the stability of this solution by linear perturbation methods. The assumed perturbation involved a sinusoidal variation in temperature and stresses in the direction parallel to the interface and exponential variation in time. The method leads to an eigenvalue problem for the exponential growth rate, stability being indicated if all the resulting eigenvalues have negative real part.

Intuitively, we might expect that the finite geometry of real systems will increase the heat flux required to initiate instability, since the finite boundaries place constraints on the temperature and stress fields that can exist within the body. The simplest such problem is that of the elastic layer in contact with a half-plane studied by Yeo and Barber (1991). They found that instability is governed by a perturbation whose spatial wavelength is related to the layer thickness.

A more challenging finite geometry problem concerns the contact of the semi-infinite strip and a rigid wall (Yeo and Barber, 1995). In this case, the finite length of the contact area causes the dominant perturbation to be non-sinusoidal, necessitating the use of a series of Papkovitch-Fadle functions and related thermoelastic functions for its representation.

The algebraic complexity of the analytical solution of the strip problem makes it clear that analytical methods are of limited use in determining the stability boundary for bodies of more general shape and necessitate the development of appropriate numerical methods. The obvious numerical approach is to simulate the transient behavior of the system by finite element or finite difference methods. However, such simulations are very computer intensive because of the small time step required to maintain stability and convergence in the solution of the transient heat conduction equation. A more practical approach is to retain the separated-variable perturbation representation and use numerical methods to discretize the equations resulting after the exponential growth factor has been cancelled. This method has already been used successfully to treat the one-dimensional problem of two contacting rods (Yeo and Barber (1994)) and gave very good results for the stability boundary with a relatively coarse discretization. In the present paper, the method is extended to investigate the instability of a two-dimensional rectangular block in thermoelastic contact with a rigid wall and the algorithm is tested against the previously published

analytical results for the strip problem.

2. The Boundary Conditions

Consider the problem shown in Fig. 1, where an elastic body Ω of rectangular shape is in frictionless thermoelastic contact with a flat rigid wall under a uniform pressure. The wall is maintained at a constant temperature T_1 . In the contact region Γ_c , heat flows into the rectangular block across a thermal contact resistance R , which depends on the local contact pressure p -- i.e. the local heat flux Q is given by

$$Q = \frac{T_1 - T}{R(p)} \quad (1)$$

where T is the temperature of Ω in Γ_c . No restriction is placed on the resistance function $R(p)$ except that it be continuous.

For the sake of simplicity, the non-contacting boundaries are assumed to be insulated for the thermal problem. For the elasticity problem, the boundaries at $y = \pm h$ are traction free.

In the steady-state, the system is in thermal and mechanical equilibrium and heat flows from the wall into the body across the contact interface. If we introduce a small transient perturbation in temperature to the steady-state, the perturbations in the prescribed boundary quantities must vanish all over the boundary except in Γ_c , where they are related by a perturbed form of Eq. (1).

We first consider a particular solution in which the perturbational quantities all take the separated-variable form in

which the field grows exponentially with time. The exponential term will then cancel in the governing equations and the perturbed boundary conditions, since these are all linear and homogeneous. The resulting equations contain the exponential growth rate as a parameter and will be discretized using the finite element method, resulting in a linear eigenvalue problem for the discrete parameters describing the spatial variation of the perturbed fields. Stability of the system is governed by the condition that all the eigenvalues should have negative real part. In practice, the first eigenvalue is always the one that determines stability.

Unless the exponential factor is explicitly included, all quantities in the following development are assumed to be functions of the spatial coordinates x_1 and x_2 only. Indices i, j, k , and l take the values 1, 2 and the summation convention applies to repeated indices of these variables only. We begin the formulation from the heat conduction equation.

2.1 Thermal Problem

The problem is time dependent only through the heat conduction equation

$$\rho c T_{,t} = K_{ij} T_{ij} \quad (2)$$

where K_{ij} is the conductivity. If we assume a perturbed temperature field of the form

$$T(x_1, x_2, t) = \theta(x_1, x_2) e^{bt}, \quad (3)$$

Eq. (2) becomes

$$K_{ij} \theta_{ij} - \rho cb \theta = 0 \text{ in } \Omega. \quad (4)$$

For the heat conduction problem, we provisionally assume that the inward heat flux q_0 is prescribed at the contact interface $\Gamma_c \subset \Gamma$, where Γ is the boundary of the body Ω . The unknown q_0 will be eliminated later, when the heat conduction and thermoelastic problem are coupled through the linearized contact resistance equation. On the rest of the boundary $\Gamma - \Gamma_c$, heat flux must vanish and hence

$$(K_{ij} \theta_{,j}) n_i = q_0 \text{ on } \Gamma_c \quad (5)$$

$$(K_{ij} \theta_{,j}) n_i = 0 \text{ on } \Gamma - \Gamma_c \quad (6)$$

where n_i is the component of the outward normal unit vector to the boundary.

The weak form of the heat conduction problem corresponding to Eq. (4) can be written.

$$\int_{\Omega} \omega_{,i} K_{ij} \theta_{,j} d\Omega + \rho cb \int_{\Omega} \omega \theta d\Omega = \int_{\Gamma} \omega K_{ij} \theta_{,j} n_i d\Gamma \text{ for all } \omega \in F, \quad (7)$$

where w is an arbitrary weighting function and the variable function space F is defined by

$$F = \{w \mid w \in H^1\} \quad (8)$$

where H^1 is a Sobolev space consisting of square-integrable functions through the first order.

Galerkin's method in discretizing the Eq. (7) with the boundary conditions (5, 6) leads to

$$\sum_{B \in \eta} \left(\int_{\Omega} N_{A,i} K_{ij} N_{B,j} d\Omega \right) \theta_B + \quad \sigma_{ij} = 0 \quad \text{in } \Omega \quad (14)$$

$$\rho c b \sum_{B \in \eta} \left(\int_{\Omega} N_A N_B d\Omega \right) \theta_B \quad \sigma_{ij} n_j = 0 \quad \text{on } \Gamma - \Gamma_c \quad (15)$$

$$= \sum_{B \in \eta_c} \left(\int_{\Gamma_c} N_A N_B d\Gamma \right) q_{0B}, \quad A \in \eta \quad \sigma_{11} = \sigma_0 \quad \text{on } \Gamma_c \quad (16)$$

$$\quad \sigma_{12} = 0 \quad \text{on } \Gamma_c \quad (17)$$

when the trial function θ in the space F is used. In the above equation, η denotes the set of the global nodes and $\eta_c \subset \eta$ the set of the contacting nodes. N_A is the shape function corresponding to node A and θ_B, q_{0B} are the nodal temperature and heat flux at node B .

In matrix notation Eq. (9) becomes

$$K\theta + bH\theta = \phi q_0 \quad (10)$$

where

$$K_{AB} = \int_{\Omega} N_{A,i} K_{ij} N_{B,j} d\Omega; \quad A, B \in \eta$$

$$H_{AB} = \rho c \int_{\Omega} N_A N_B d\Omega, \quad A, B \in \eta$$

$$\phi_{AB} = \int_{\Omega} N_A N_B d\Gamma \quad A \in \eta, \quad B \in \eta_c.$$

and q_0 is a column vector consisting of the nodal values of heat flux at nodes $B \in \eta_c$.

2.2 Contact Pressure

An essentially similar procedure is adopted for the mechanical part of the problem. For the contact problem, therefore, we provisionally assume that the normal stress $\sigma_n = \sigma_0$ is prescribed at the frictionless contact plane $\Gamma_c \subset \Gamma$. At the rest of the boundary, tractions vanish, hence the strong statement of the present problem is

with the constitutive relation

$$\sigma_{ij} = E_{ijkl} (\epsilon_{kl} - \alpha_{kl} \theta) \quad (18)$$

where E_{ijkl}, α_{ij} are the elastic constant and thermal expansion coefficient, respectively. ϵ_{ij} denotes the Cauchy strain tensor and

$$\epsilon_{ij} = \frac{1}{2} (u_{i,j} + u_{j,i}). \quad (19)$$

The equivalent weak form of Eqs. (14,18) is

$$\int_{\Omega} w_{i,j} E_{ijkl} u_{k,l} d\Omega =$$

$$\int_{\Omega} w_{i,j} E_{ijkl} \alpha_{kl} \theta d\Omega + \quad (20)$$

$$\int_{\Gamma} w_i (\sigma_{ij} n_j) d\Gamma \quad \text{for all } w_i \in F_i.$$

Galerkin's method to discretize Eq. (20) with the boundary conditions (15-17) again leads us to the following equation

$$\sum_{B \in \eta} \left(\int_{\Omega} N_{A,i} E_{ijkl} N_{B,j} d\Omega \right) U_{kB} =$$

$$\sum_{B \in \eta} \left(\int_{\Omega} N_{A,i} E_{ijkl} \alpha_{kl} N_B d\Omega \right) \theta_B \quad (21)$$

$$+ \sum_{B \in \eta_c} \left(\int_{\Gamma_c} N_A N_B d\Gamma \right) n_i \sigma_{0B}, \quad A \in \eta$$

which can be written in matrix notation as

$$LU = F\theta + f\sigma_0 \quad (22)$$

where

$$L_{pq} = \int_{\Omega} N_{A,k} E_{ijkl} N_{B,l} d\Omega ;$$

$$p = G(i, A), \quad q = G(j, B) \quad (23)$$

$$F_{pB} = \int_{\Omega} N_{A,k} N_{ijkl} \alpha_{jl} N_B d\Omega \quad (24)$$

$$f_p = \int_{\Gamma_c} N_A N_B d\Gamma n_i \quad (25)$$

and $p=G(i,A)$ is the global equation number corresponding to the node A and the i th degree of freedom (here $i=1, 2$). The contact stress can now be calculated from Eq. (22), which is conveniently rearranged in the partitioned form

$$\begin{bmatrix} L_{11} & L_{12} \\ L_{21} & L_{22} \end{bmatrix} \begin{bmatrix} U_1 \\ U_2 \end{bmatrix} = \begin{bmatrix} F_1 \\ F_2 \end{bmatrix} \begin{bmatrix} \theta \end{bmatrix} + \begin{bmatrix} f_1 & f_2 \end{bmatrix} \begin{bmatrix} \sigma_0 \end{bmatrix} \quad (26)$$

where U_1 consists of the nodal normal displacements at the contact area. The order of the equation is rearranged so that L maintains symmetry, which requires that the order of the contact nodes be same as the order of the corresponding equilibrium equations, as a result of which the matrix is partitioned. Noting that $U_1 = \{0\}$ and $f_2 = \{0\}$ and eliminating U_2 in the above equation we have

$$\sigma_0 = S\theta \quad (27)$$

where

$$S = f_1^{-1} (L_{12}L_{22}^{-1}F_2 - F_1). \quad (28)$$

2.3 Stability Analysis

Eq. (1) defines the heat flux Q across the thermal contact resistance R , which is a function of the local pressure p . If the steady state heat flux Q_0 and pressure p_0 are constant throughout the contact plane, a linear perturbation of Eq. (1) about the steady-state can be written in the matrix form

$$-P\theta = -Q_0R' \sigma_0 + R_0q_0 \quad (29)$$

where P is a matrix whose elements are zeros except for a unity in each row, which must be located in correspondence with that of the node corresponding to the row in the column vector θ . R' denotes the derivative of the contact resistance with respect to variations in contact pressure about the steady-state value. The row dimension is the number of the nodes in the set η_c and the column dimension is the number of the nodes in the set η .

Using Eqs. (10,27) to eliminate σ_0, q_0 in Eq.(29) yields the linear eigenvalue problem

$$A\theta = bR_0H\theta \quad (30)$$

where

$$A = Q_0R' \phi S - R_0K - \phi P. \quad (31)$$

Thus, if the steady-state quantities Q_0, R', R_0 are known, the stability of the thermoelastic system can be determined by solving the linear eigenvalue problem (29) for the exponential growth rate b . Stability

requires that all the eigenvalues of this equation have negative real part.

3. Results and Conclusions

To illustrate the use of the algorithm and to assess its accuracy and convergence, we consider the two-dimensional system of Fig. 1, in which a rectangular block of width $2h$ and length l is pressed against a rigid frictionless wall which is maintained at uniform temperature T_1 . The boundary at $x=l$ is subject to uniform pressure p_0 and is insulated. The boundaries at $y=\pm h$ are traction-free and insulated. The block is assumed to be isotropic, homogeneous and linear elastic and plane strain conditions were used in the analysis.

The block can be characterized by the dimensionless aspect ratio

$$r = \frac{l}{h} \quad (32)$$

Two limiting solutions are of interest and have already been investigated by analytical means. When $r \rightarrow 0$, the block reduces to an infinite layer in contact with a rigid wall, which is a special case of the layer solution due to Yeo and Barber (1991). The eigenfunction in this case will be sinusoidal in the y -direction. At the other extreme, $r \rightarrow \infty$, the block reduces to the semi-infinite strip in contact on an end face, which was considered by Yeo and Barber (1995).

The rectangular block and the boundary conditions are symmetrical about the plane $y=0$, but it does not

necessarily follow that the governing unstable perturbation will exhibit the same symmetry. In fact, the resulting eigenvalue problem can be partitioned into a symmetric and an antisymmetric problem and the stability boundary for the system will be determined by whichever of these goes unstable at the lowest steady-state heat flux Q_0 . Invoking this partition, we solve the symmetric and antisymmetric problems separately, discretizing the region $0 < y < h$ only. For the symmetric modes, the appropriate symmetry conditions at $y=0$ are then $u_y=0$, $\sigma_{xy}=0$, $q_y=0$ whereas for the anti-symmetric mode they are $\sigma_{yy}=0$, $u_x=0$, $T=0$.

If the aspect ratio is reasonably large, we anticipate that the perturbed fields will be concentrated near the contact boundary and will decay with x . In the limit of the strip, the dominant term in the eigenfunction decays exponentially with x (Yeo and Barber, 1995). To take advantage of this behaviour, three node triangular elements were used to develop the discretization of Fig. 2, in which greater resolution of the eigenfunction is obtained near to the contact boundary.

The problem can be completely characterized by the aspect ratio r , Poisson's ratio ν (here taken as $1/3$) and the two dimensionless parameters

$$R^* = \frac{R_0 K}{h} ; Q^* = -QR'2\mu\alpha(1+\nu) \quad (33)$$

introduced by Yeo and Barber (1995), which can be interpreted as dimensionless contact resistance and heat flux respectively. μ is the shear modulus.

3.1 Results

Results were obtained for a wide range of values of r , R^* , Q^* with a view to determining the progress of the leading eigenvalue b into the positive half-plane and hence the stability boundary for the system. In all cases, it was found that unstable perturbations were always characterized by real eigenvalues and hence that the stability boundary is determined by the passage of the first such eigenvalue through the origin. Similar results were obtained by Barber (1980, 1987) for the contact of a rod and a deformable half-plane respectively against a perfectly-conducting rigid wall and it is speculated that this will always be the case for a thermoelastic contact system in which one of the two contacting bodies is a perfect conductor. However, the fact in a general theorem has not been able to be proved and is left as a challenge to the reader.

Determination of the stability boundary is greatly simplified when it is associated with a real eigenvalue, since we can then set $b=0$ in Eq. (30), implying $A\theta=0$. Substituting for A from Eq. (31), we then obtain a new linear eigenvalue problem for Q^* which is the minimum dimensionless heat flux for instability.

Fig. 3.4 show the temperature distribution along the contact plane associated with the three lowest eigenvalues Q^* in the symmetric and antisymmetric modes respectively, for $r=1$ and $R^*=1$. The first symmetric mode determines the stability of the system and this is also found to be the case for other values of aspect ratio. All the ei-

genfunctions have roughly sinusoidal form and the 'wavelength' of the dominant eigenfunction for $r=1$ is approximately equal to the contact length.

The stability boundary is plotted as a function of the aspect ratio in Fig. 5 for $R^*=1.0$. Very little change in the critical dimensionless heat flux Q^* occurs for increase in the aspect ratio beyond $r \approx 1$. The limiting value of Q^* for large r agrees within 3% with that obtained analytically by Yeo and Barber (1995) for the semi-infinite strip.

The effect of dimensionless thermal contact resistance R^* is explored in Fig. 6, where the stability for the first symmetric and antisymmetric modes is presented as a function of R^* for $r=5$. The results are in good agreement with those calculated analytically for the semi-infinite strip.

When the aspect ratio $r \rightarrow 0$, the system approaches the limit of an infinite layer in contact with a rigid wall and analytical solutions show that the stability boundary is determined by an eigenfunction which is sinusoidal with a wavelength that is related to the layer thickness (Yeo and Barber, 1991). For small but finite aspect ratio, the number of waves in the dominant eigenfunction increases as r is decreased. Fig. 7,8 show the eigenfunctions corresponding to the three lowest eigenvalues in the symmetric and antisymmetric modes respectively for $r=0.1$ and $R^*=1$.

3.2 Conclusions

The main advantage of the finite element method presented herein is that

the exponential growth rate b , the positive real part of which indicates instability of the system, can be obtained from the linear eigenvalue problem if R^* and Q^* are given.

The formulation presented can be directly used in the more general problem of the thermoelastic contact of two deformable bodies with the non-uniform steady-state quantities along the contact plane.

Finally, this study may be considered as a stepping stone to develop a numerical method for the more challenging problems of frictionally-excited thermoelastic instability between two sliding bodies.

References

- [1] J.R. Barber, J. Dundurs and M. Comninou, 1980, "Stability considerations in thermoelastic contact," *ASME J. Appl. Mech.*, Vol. 47, pp. 871-874.
- [2] J.R. Barber, 1986, "Non-uniqueness and stability for heat conduction through a duplex heat exchanger tube," *J. Thermal Stresses*, Vol. 9, pp. 69-78.
- [3] J.R. Barber, 1981, "Stability of thermoelastic contact for the Aldo model," *ASME J. Appl. Mech.*, Vol. 48, pp.555-558.
- [4] J.R. Barber, 1987, "Stability of thermoelastic contact," *Institution of Mechanical Engineers*, International Congress on Tribology, London, pp.981-986.
- [5] J.R. Barber and R. Zhang, 1988, "Transient behaviour and stability for the thermoelastic contact of the two rods of dissimilar materials," *Int. J. Mech. Sci.*, Vol. 30, pp. 691-704.
- [6] T.A.Dow and R.A.Burton, 1972, "Thermoelastic instability of sliding contact in the absence of wear", *Wear*, Vol.19, pp. 315-328.
- [7] O.Richmond and N.C.Huang, 1977, "Interface stability during unidirectional solidification of a pure metal", Proc. 6th.Canadian Congress of Applied Mechanics, Vancouver., pp.453-454.
- [8] Taein Yeo and J.R. Barber, 1991, "Stability of thermoelastic contact of a layer and a half-plane," *J. Thermal Stresses*, Vol. 14, pp. 371-388.
- [9] Taein Yeo and J.R. Barber, 1994, "Finite element analysis of thermoelastic contact stability," *ASME, J. Appl. Mech.*, Vol. 61, pp. 919-922.
- [10] Taein Yeo and J.R.Barber, 1995, "Stability of a semi-infinite strip in thermoelastic contact with a rigid wall," *Int. J. Solids and Structures*, Vol. 32, No. 3/4, pp. 553-567.

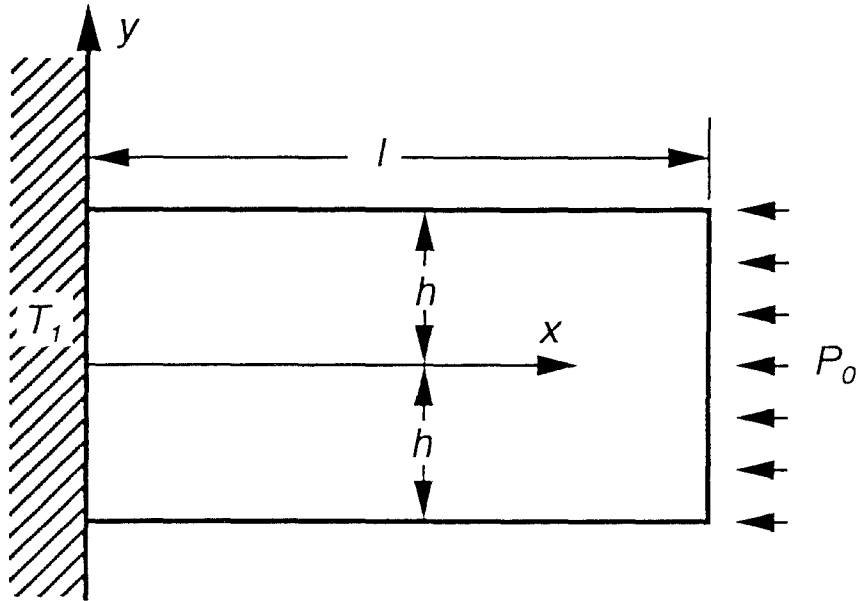


Fig.1 A rectangular block contacting a rigid wall.

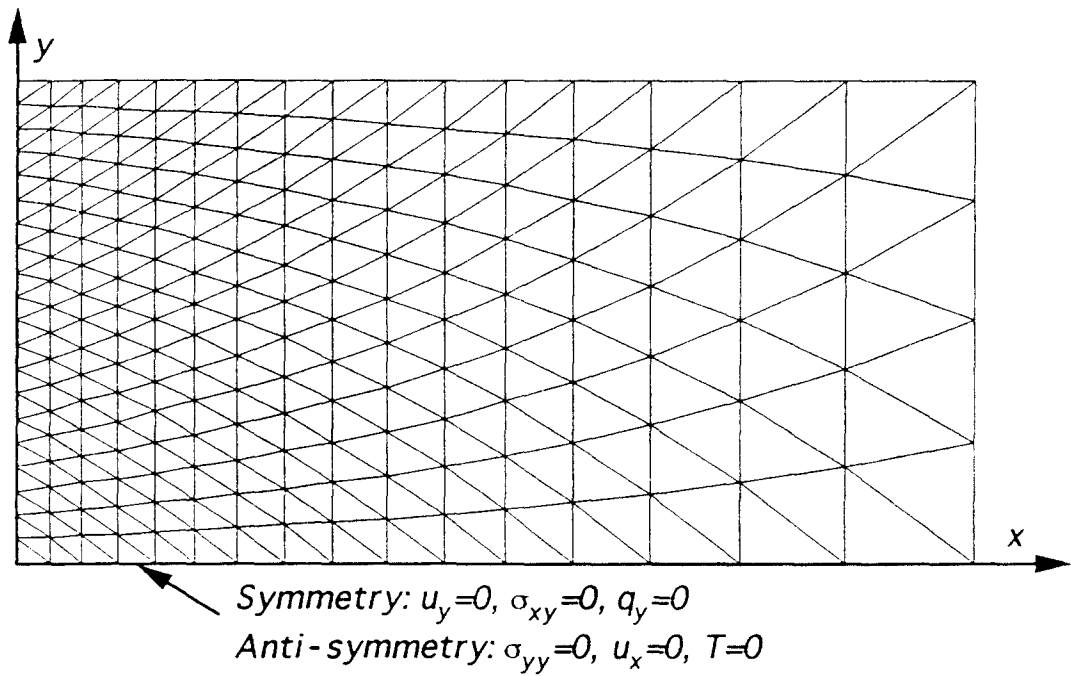


Fig.2 Mesh used in analysis. Due to symmetry, only one half is discretized.

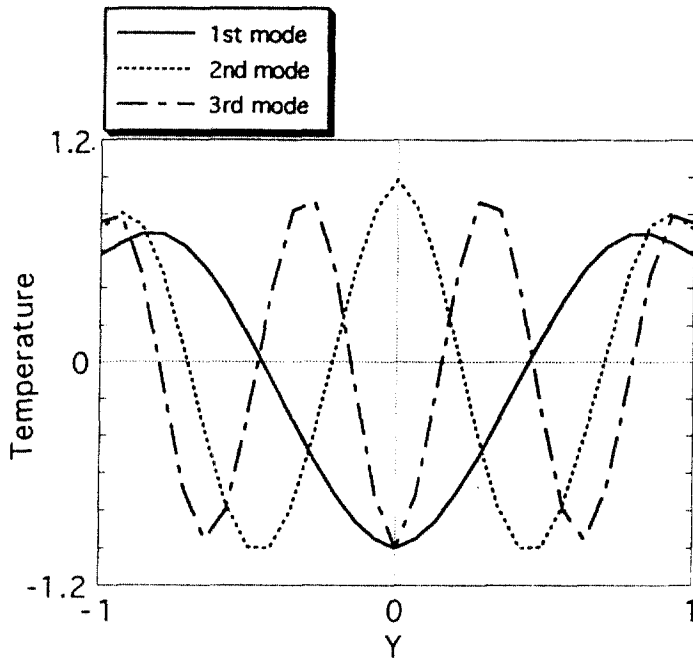


Fig.3 Symmetric modes of temperature perturbation. $\nu=1/3$, $R^*=1.0$, $r=1.0$

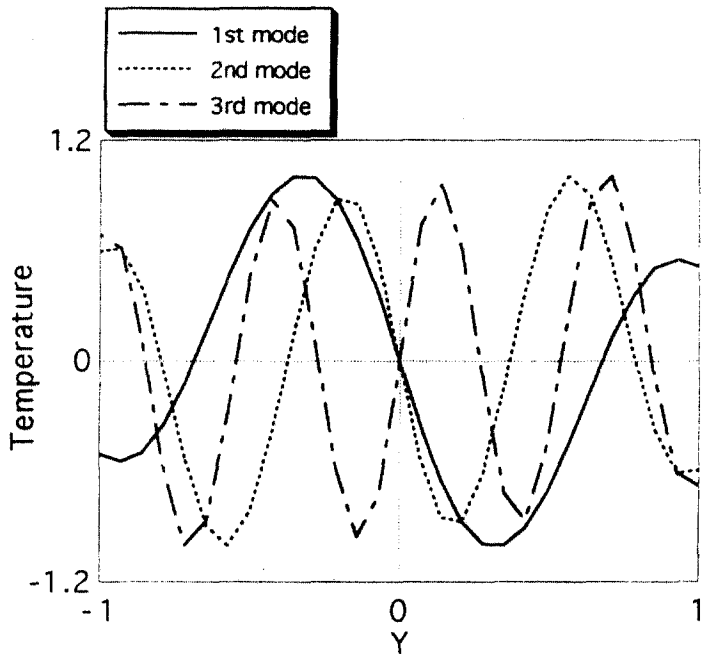


Fig.4 Anti-symmetric modes of temperature perturbation. $\nu=1/3$, $R^*=1.0$, $r=1.0$

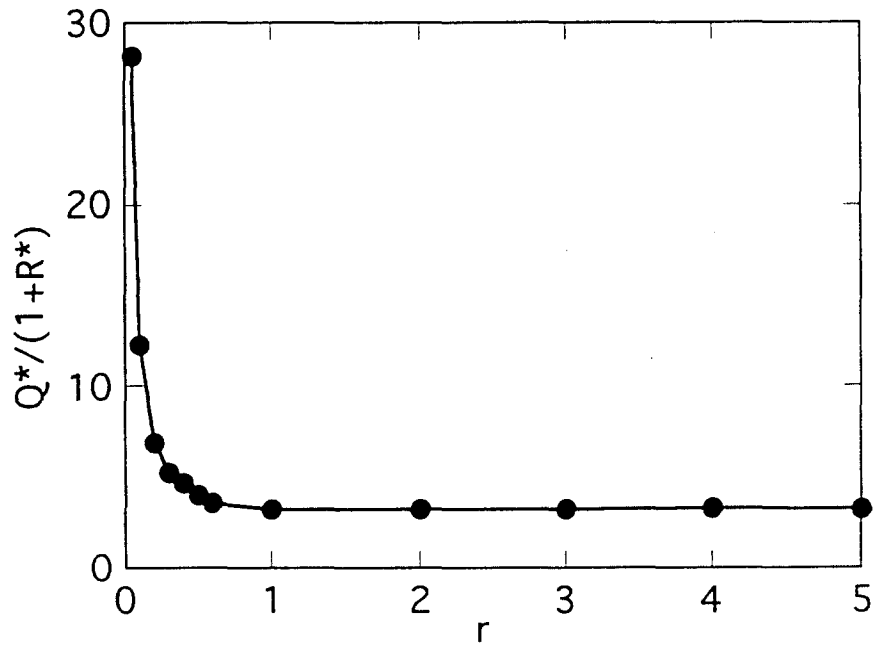


Fig.5 Stability boundary as a function of the aspect ratio r . $\nu=1/3$, $R^*=1.0$

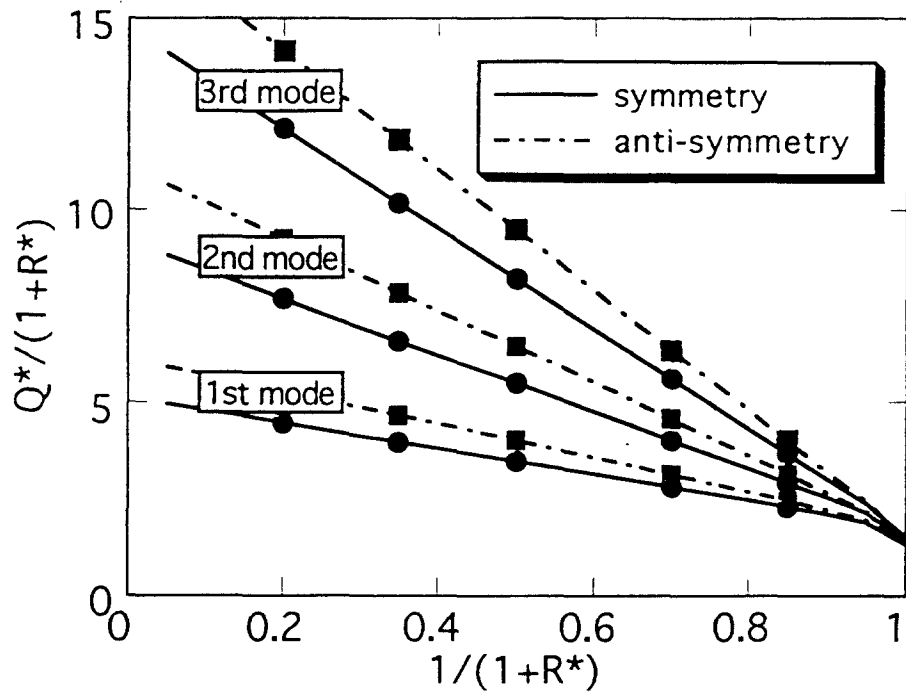


Fig.6 Stability boundary of the rectangular block contacting the rigid wall.
 $\nu=1/3$, $R^*=1.0$

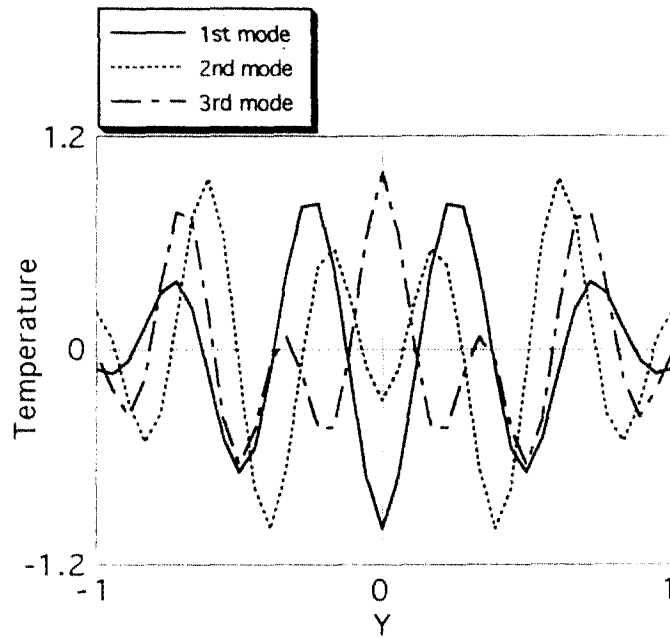


Fig.7 Symmetric modes of temperature perturbation. $\nu=1/3$, $R^*=1.0$, $r=0.1$

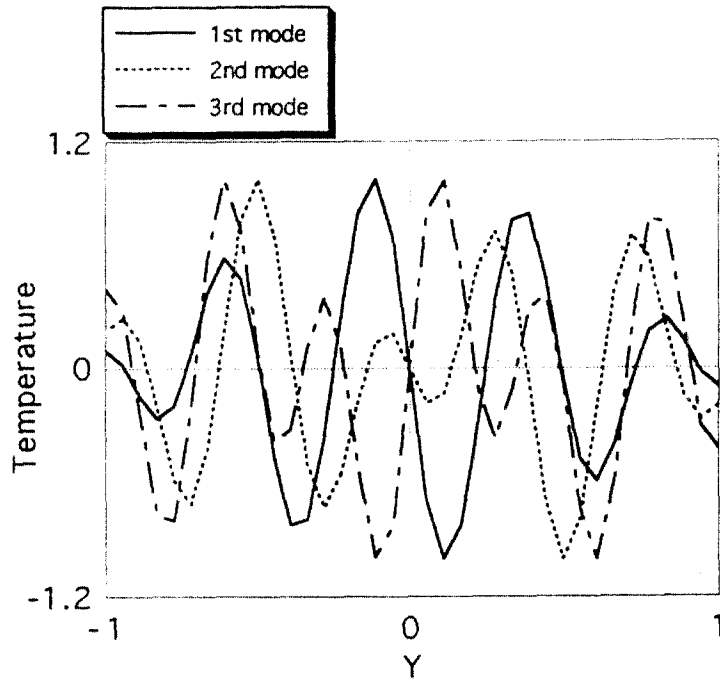


Fig.8 Anti-symmetric modes of temperature perturbation. $\nu=1/3$, $R^*=1.0$, $r=0.1$